Published online 16 April 2015

Nucleic Acids Research, 2015, Vol. 43, No. 14 ***e92***
doi: 10.1093/nar/gkv338

Thioflavin T as a fluorescence probe for monitoring RNA metabolism at molecular and cellular levels

Shinya Sugimoto[1,2,*], Ken-ichi Arita-Morioka[1], Yoshimitsu Mizunoe[2], Kunitoshi Yamanaka[1] and Teru Ogura[1,*]

[1]Department of Molecular Cell Biology, Institute of Molecular Embryology and Genetics, Kumamoto University, Chuo-Ku, Kumamoto 860-0811, Japan and [2]Department of Bacteriology, The Jikei University School of Medicine, Minato-Ku, Tokyo 105-8461, Japan

Received December 7, 2014; Revised March 16, 2015; Accepted April 2, 2015

ABSTRACT

The intrinsically stochastic dynamics of mRNA metabolism have important consequences on gene regulation and non-genetic cell-to-cell variability; however, no generally applicable methods exist for studying such stochastic processes quantitatively. Here, we describe the use of the amyloid-binding probe Thioflavin T (ThT) for monitoring RNA metabolism *in vitro* and *in vivo*. ThT fluoresced strongly in complex with bacterial total RNA than with genomic DNA. ThT bound purine oligoribonucleotides preferentially over pyrimidine oligoribonucleotides and oligodeoxyribonucleotides. This property enabled quantitative real-time monitoring of poly(A) synthesis and phosphorolysis by polyribonucleotide phosphorylase *in vitro*. Cellular analyses, in combination with genetic approaches and the transcription-inhibitor rifampicin treatment, demonstrated that ThT mainly stained mRNA in actively dividing *Escherichia coli* cells. ThT also facilitated mRNA metabolism profiling at the single-cell level in diverse bacteria. Furthermore, ThT can also be used to visualise transitions between non-persister and persister cell states, a phenomenon of isogenic subpopulations of antibiotic-sensitive bacteria that acquire tolerance to multiple antibiotics due to stochastically induced dormant states. Collectively, these results suggest that probing mRNA dynamics with ThT is a broadly applicable approach ranging from the molecular level to the single-cell level.

INTRODUCTION

Defining temporal fluctuations in gene expression in specific cells within organisms ranging from bacteria to humans will provide molecular insights into diverse biological processes, including morphogenesis, development, differentiation and adaptation to environmental stresses (1–6). Recently, several techniques have become available that enable investigation of this central issue in individual living cells, rather than depending upon the averaged properties of large populations (7–10). Unfortunately, there are still no general methods for meeting this important challenge.

Bacterial persistence is an example of a biological process that results from the fluctuations in gene expression in specific cells (11,12). Bacterial persistence was initially reported in 1944 (13) and is currently being studied extensively (11,14–17). Persisters are slow-growing cells that tolerate treatment with multiple drugs. Persisters are rare bacterial cells that form stochastically and are thus genetically identical to the majority of the bacterial population (11,12). In persister cells, type II toxin–antitoxin (TA) systems are believed to be important for inducing the resting state. Ectopically induced toxins of TA modules inhibit replication, transcription or translation, leading to the arrest of cell growth and drug tolerance (18). Understanding the genesis of bacterial persisters is important not only for understanding bacterial physiology, but also for the eradication of these multi-drug tolerant bacteria. Distinguishing persister cells from normal cells has been challenging because they are minority populations (ranging from 10^{-6} to 10^{-1}) and a lack of information concerning persister-specific gene expression profiles exists. However, such information can be attained using recently developed imaging techniques such as microscopes, microfluidics and flow cytometry (19). Fluorescent protein-based reporter systems have also been developed to monitor persister cells (11,17,20). However, non-genetic approaches are also strongly desired in the case of studying organisms in which genetic manipulation has not yet been established and conventional fluorescent protein reporter systems do not provide adequate information.

Thioflavin T (ThT; 4-(3,6-dimethyl-1,3-benzothiazol-3-ium-2-yl)-N,N-dimethylaniline chloride), is a well-known fluorescence probe used for detecting amyloid fibrils (21).

*To whom correspondence should be addressed. Tel: +81 3 3433 1111; Fax: +81 3 3436 3166; Email: ssugimoto@jikei.ac.jp
Correspondence may also be addressed to Teru Ogura. Tel: +81 96 373 6578; Fax: +81 96 373 6582; Email: ogura@gpo.kumamoto-u.ac.jp

Upon binding to fibrils, ThT displays a dramatic shift of excitation maximum (from 385 to 450 nm) and emission maximum (from 445 to 492 nm) (22,23), resulting in an increase in ThT fluorescence intensity by several orders of magnitude. This property makes ThT a sensitive and efficient indicator that enables quantitative real-time observations of amyloid fibril formation *in vitro*. Recently, ThT was used as a selective fluorescent sensor for the human telomeric G-quadruplex, a 4-stranded nucleic acid structure formed by the stacking of Hoogsteen base-paired coplanar guanines, termed G-quartets (24–26). Although the actual roles and functional mechanisms of G-quadruplexes remain unclear, they may serve as drug targets for regulating gene expression, as they are found abundantly in functional genomic regions such as in the promoter regions of proto-oncogenes and untranslated regions of mRNAs (27). ThT and its derivatives may be used as highly sensitive G-quadruplex-sensing probes for diagnostic and therapeutic applications (25).

Here, we show that ThT can be used as an RNA-binding probe for monitoring RNA metabolism in real-time, both *in vitro* and *in vivo*. We further demonstrate that this fluorescent probe can be used to visualize transitions between normal cells and persister cells and to profile mRNA metabolism at the single-cell level in *Escherichia coli* and other bacteria. Our present work provides a very simple, efficient and quick method for analysing the mRNA dynamics. Thus, we anticipate that this assay will be widely used in the fields of nucleic acid research, enzymology, microbiology and single-cell imaging.

MATERIALS AND METHODS

Chemicals

Adenosine 5′-diphosphate (ADP), poly(A), poly(dA), poly(C), poly(G), poly(U), kanamycin (Km), rifampicin (Rfp) and Thioflavin S (ThS) were purchased from Sigma. DAPI was from Dojindo Laboratory, FM4–64 was from Life Technologies, isopropyl-1-thio-β-D-galactopyranoside (IPTG) was from Nacalai Tesque and ThT was from AAT Bioquest. *E. coli* total RNA was purified using RNeasy Protect Bacteria kit (Qiagen). Oligoribonucleotides (>90% purity) and oligodeoxyribonucleotides (>95% purity) were synthesized by GeneDesign (Supplementary Table S1).

Bacterial strains and plasmids

Bacterial strains used in this study (Supplementary Table S2) were grown at 30 or 37°C in LB medium containing appropriate antibiotics (50 μg/ml kanamycin or 30 μg/ml chloramphenicol). In the cases of *E. coli* MG1693, SK5691 (28,29) and JEFZ1 (30), 20 μg/ml thymine was supplemented into the medium. *Brevibacillus choshinensis* NCMO2 (31) was cultured in brain heart infusion (BHI) medium supplemented with 50 μg/ml neomycin. Plasmids used in this study are also listed in Supplementary Table S2. The *pnp* gene encoding wild-type polyribonucleotide phosphorylase ($PNPase^{WT}$) was amplified from *E. coli* JM109 genomic DNA using the specific primers harbouring NdeI and BamHI restriction sites (Supplementary Table S3) and cloned into pET28b (Novagen) plasmid using NdeI and BamHI restriction sites. A mutant of *pnp* encoding $PNPase^{R398D/R399D}$ was generated by polymerase chain reaction mutagenesis using the indicated oligonucleotide primers (Supplementary Table S3) and standard cloning techniques and was verified by sequencing.

Purification of recombinant proteins

N-terminally His-tagged $PNPase^{WT}$ and $PNPase^{R398D/R399D}$ were expressed in *E. coli* BL21(DE3) and purified at 4°C by nickel-affinity chromatography with a HisTrap HP column (GE Healthcare) or Proteino Ni-TED (MACHEREY-NAGEL) according to manufactures' instructions. Peak fractions were collected and dialyzed against buffer A (40 mM Hepes (pH 7.4), 150 mM KCl and 20 mM $MgCl_2$) at 4°C overnight. The dialysates were stored at −80°C. Protein concentrations were determined with a Bradford assay kit (BioRad).

In vitro ThT binding assay

The indicated concentrations of *E. coli* total RNA, poly(A), poly(G), poly(C), poly(U), poly(dA), oligoribonucleoides and oligodeoxyribonucleotides were incubated with 25 μM ThT in buffer A for several minutes at room temperature. Reaction volumes were 400 μl. Emission spectra between wavelengths of 450 to 650 nm were recorded on a Hitachi F-7000 fluorescence spectrophotometer with the excitation wavelength at 438 nm. If required, ThS was used instead of ThT. All experiments were repeated at least three times to ensure accuracy. Averaged values with standard deviations were calculated.

In vitro poly(A) synthesis and phosphorolysis

For analysis of poly(A) synthesis, the indicated concentrations of $PNPase^{WT}$ or $PNPase^{R398D/R399D}$ were incubated with 1 mM ADP and 25 μM ThT. Real-time increases in fluorescence were recorded at 25°C by spectrofluorometer with the excitation wavelength at 438 nm and emission wavelength at 491 nm. For analysis of poly(A) phosphorolysis, real-time changes of ThT fluorescence intensity with the excitation wavelength at 438 nm and emission wavelength at 491 nm was monitored in the presence of 1 μM $PNPase^{WT}$ or $PNPase^{R398D/R399D}$, 20 μg/ml poly(A), 10 mM potassium phosphate and 25 μM ThT in buffer A at 25°C. Reaction volumes were 600 μl. All experiments were repeated at least three times to ensure accuracy. If required, averaged values with standard deviations were calculated.

Determination of ADP concentration

The indicated concentrations of ADP were incubated with 200 nM $PNPase^{WT}$ and 25 μM ThT in buffer A. Reaction volumes were 600 μl. The kinetics of poly(A) synthesis was monitored at 25°C as the function of the increases in fluorescence intensity with the excitation wavelength at 438 nm and emission wavelength at 491 nm. The fluorescence intensities recorded at 20 min were plotted against the ADP concentrations. Approximation straight line and its formula

with a correlation coefficient were calculated with Microsoft Excel 2010. All experiments were repeated at least three times. If required, averaged values with standard deviations were calculated.

Poly(A) synthesis using *E. coli* crude extracts

Escherichia coli strains MC4100(DE3) (wild-type) (32), BM271(DE3) (Δ*dnaK*52::Cm^R) (33,34), MG1693 (wild-type) and SK5691 (*pnp-7*) (28) were grown in LB medium at 30°C with shaking. For MG1693 and SK5691, 20 μg/ml thymine was supplemented. At the exponential growth phase, *E. coli* cells were collected by centrifugation at 15 000 × *g* for 10 min at 4°C and stored at −30°C. The bacterial pellets were washed twice with buffer A, resuspended into buffer A and then disrupted by sonication on ice. Soluble proteins were recovered by ultracentrifugation at 100 000 rpm for 10 min at 4°C using a Beckman TLA100 rotor (Beckman-Coulter). Soluble proteins were freshly prepared for each experiment. Protein concentrations were determined with a Bradford assay kit (BioRad).

Escherichia coli cytoplasmic soluble proteins (0.5 mg/ml) were incubated in buffer A supplemented with 25 μM ThT at 30°C for 3 h in the presence or absence of 5 mM ADP. Reaction volumes were 400 μl. Emission spectra between wavelengths of 450 to 650 nm were recorded using an excitation wavelength of 438 nm. All experiments were repeated at least three times and averaged values with standard deviations were represented.

ThT binding assay for bacterial whole cells

Bacterial strains were grown in LB or BHI (only for *B. choshinensis* cells) medium containing appropriate antibiotics or thymine at 37°C overnight. The overnight culture was 1000-fold diluted into fresh appropriate medium. At the indicated time points, bacterial cells were harvested, washed twice with phosphate buffered saline (PBS) and their wet weights were recorded. Bacterial cells (2.3 mg wet weight) were incubated with 25 μM ThT in PBS (600 μl) at room temperature for at least 5 min. Emission spectra between wavelengths of 450 to 650 nm were recorded using an excitation wavelength of 438 nm. All experiments were repeated at least three times and averaged values with standard deviations were represented.

Microscopy

Bacterial cells grown in appropriate medium at 37°C were harvested at the indicated time points by centrifugation at 10 000 × *g* for 5 min and washed twice with PBS. The harvested cells were stained with 25 μM ThT. If required, the cells were further stained with 2 μg/ml DAPI and 1 μM FM4-64 for several minutes at room temperature. Five microliters of the suspension were dropped on a glass slide and covered with a cover glass. For distinguishing normal cells from persisters, *E. coli* MG1655 *rpoS::mcherry* cells (kindly gifted by Dr Gerdes) (11) at the indicated growth phases were stained with 25 μM ThT. These cells were observed under fluorescence microscopy (Nikon) equipped with B2 (excitation filter, 450–490 nm; barrier filter, 520 nm), UV-1A (excitation filter, 360–370 nm; barrier filter, 420 nm) and G2A (excitation filter, 510–560 nm; barrier filter, 590 nm) filters. Intensities of ThT fluorescence and mCherry fluorescence of individual cells were determined using Image J software (version 1.48).

Real-time imaging of bacterial growth with ThT

To check the effect of ThT on the growth of bacterial strains, ThT was supplemented into media at the indicated concentrations and bacterial growth was monitored at 37°C by measuring optical density at 660 nm. Small aliquots (5 μl) were taken from the culture and spotted on a slide glass. Cell morphology and ThT fluorescence were observed under fluorescence microscopy.

RESULTS

ThT binds to RNA purine bases

ThT, a typical probe for amyloid fibrils, binds to human telomeric G-quadruplex DNA with a fluorescent light-up signal change (24–26). Here, we examined whether ThT binds to DNA and RNA lacking specific target sequences. For this purpose, we used genomic DNA and total RNA both of which were purified from the *E. coli* strain K-12. ThT exhibited higher fluorescence in the presence of *E. coli* total RNA than in the presence of *E. coli* genomic DNA (Figure 1A). In addition, this light-up probe quantitatively detected RNA (Figure 1B and C).

Mohanty *et al.* proposed ThT-binding modes with G-quadruplexes that were revealed by performing molecular dynamics simulations (25). They proposed that π stacking from the rigid aromatic rings of ThT and the G-quartet are important for complex formation. Thus, we measured whether ThT exhibits high fluorescence intensity in the presence of four homo-polymeric ribonucleic acids to determine the RNA-base module specificity of ThT. Remarkably, ThT exhibited high fluorescence in the presence of poly(A) and poly(G), but not in the presence of either poly(U) or poly(C), indicating that ThT preferentially binds to purine bases (Figure 1D). In addition, ThT bound to poly(A) and poly(G) quantitatively (Figure 1E, F and Supplementary Figure S1). Interestingly, ThS, another well-known amyloid-binding probe, did not show a significant fluorescence increase in the presence of poly(A) (Supplementary Figure S2A).

ThT showed higher fluorescence intensities when interacting with *E. coli* total RNA than with *E. coli* genomic DNA, suggestive of higher-affinity interactions (Figure 1A). This observation may be due to differences in the purine base contents and the lengths between RNA and DNA samples used for assays. To test these possibilities, we compared ThT fluorescence when incubated with either commercial poly(A) or poly(dA), both of which were enzymatically synthesized and had lengths that were therefore not identical. ThT exhibited higher fluorescence in the presence of poly(A) than in the presence of poly(dA) (Figure 1G). Furthermore, ThT fluorescence in the presence of synthetic oligoribonucleotides $(A)_{50}$ and $(A)_{25}$ was markedly higher than in the presence of synthetic oligodeoxyribonucleotides $(dA)_{50}$ and $(dA)_{25}$, in a length-dependent manner (Figure 1H). ThT-binding was greatly

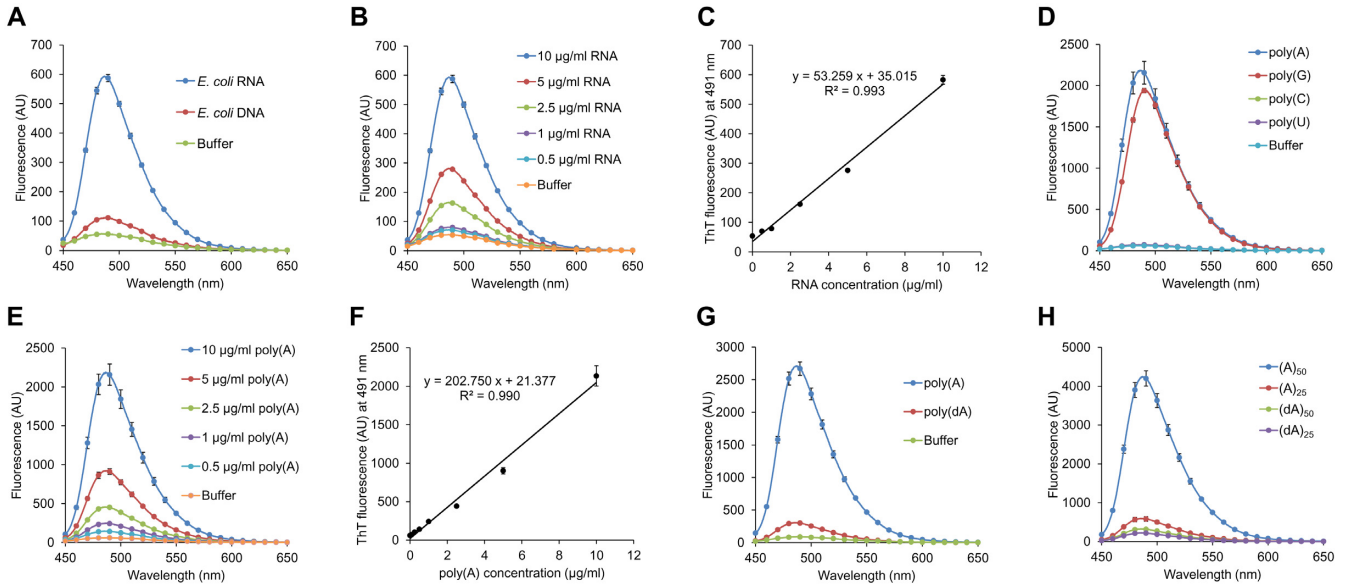

Figure 1. ThT quantitatively binds to purine bases of RNA. (**A** and **B**) ThT fluorescence spectra of RNA (10 μg/ml *Escherichia coli* total RNA) and DNA (10 μg/ml *E. coli* genomic DNA) were measured. (**C**) Fluorescence intensities at 491 nm recorded in (**B**) were plotted against RNA concentrations. Approximation straight line and its formula are shown with a correlation coefficient. (**D**, **G** and **H**) ThT fluorescence spectra of poly(A), poly(G), poly(C), poly(U), poly(dA), oligoribonucleotides $(A)_{50}$ and $(A)_{25}$, and oligodeoxyribonucleotides $(dA)_{50}$ and $(dA)_{25}$ were measured at 10 μg/ml. (**E**) ThT fluorescence spectra of poly(A) were measured at the indicated concentrations. (**F**) Fluorescence intensities at 491 nm recorded in (**E**) were plotted against poly(A) concentrations. The approximation line and its formula are shown with a correlation coefficient. Data points represent the means and standard deviations of results from three independent experiments. The standard deviation is less than that corresponding to the size of the symbol if no error bars are seen.

reduced for $(A)_{50}$ after pre-treatment at the increased temperatures (Supplementary Figure S3). In contrast, ThT-binding to $(dA)_{50}$ was not affected by pre-heat treatment (Supplementary Figure S3), suggesting that $(A)_{50}$ could form a certain secondary structure, such as parallel duplex (35) and that a minimal length of RNA molecules may be required for its formation.

Renaud de la Faverie *et al.* recently reported that ThT showed higher fluorescence intensities when interacting with G-quadruplex structures (26). Here, we also tested the ThT-binding to DNA and RNA sequences forming duplex, parallel duplex, triplex and G-quadruplex structures (Supplementary Table S1). ThT showed the highest fluorescence intensities when bound to G-quadruplex sequences (Supplementary Figure S4A and B). These results were consistent with the recent publication (26). Of note, ThT also exhibited higher fluorescence intensities when interacting with DNA than with RNA for many other sequences, except for $(A)_{50}$ and $(dA)_{50}$ (Supplementary Figure S4C and D). Taken together, these results indicate that ThT binds preferentially to RNA or DNA depending upon their sequence, length and structure.

Application of ThT in characterizing a bifunctional RNA metabolic enzyme, polyribonucleotide phosphorylase

The strong increase in ThT fluorescence intensity upon RNA binding observed (Figure 1) suggested that ThT is a sensitive reporter that could eliminate the need for washing away unbound fluorophores, thereby enabling real-time measurements of RNA synthesis and phosphorolysis. Thus, poly(A) synthesis and phosphorolysis were analysed in real-time by using purified *E. coli* PNPase, a bifunctional enzyme with 5′ to 3′ oligonucleotide polymerase activity and 3′ to 5′ phosphorolytic exoribonuclease activity (36). ThT facilitated the detection of poly(A) synthesis in reactions at 25°C in a time-dependent manner (Figure 2A) and the initial rates of ThT fluorescence intensity increases were highly correlated with the concentration of wild-type PNPase ($PNPase^{WT}$) used ($R^2 = 0.994$; Figure 2B). In contrast, no detectable increase in ThT fluorescence was observed in the presence of a PNPase mutant ($PNPase^{R398D/R399D}$) lacking poly(A) synthesis activity (37) (Figure 2C), indicating that the increase in ThT fluorescence observed reflected poly(A) synthesis. Furthermore, ThT can be used to evaluate the poly(A) synthesis activity of PNPase using not only purified proteins, but also crude *E. coli* lysates (Supplementary Figure S5). Phosphorolysis of poly(A) driven by PNPase was analysed by measuring ThT fluorescence and the fluorescence intensities measured gradually decreased when poly(A) was incubated in the presence of $PNPase^{WT}$ (Figure 2D). In contrast, only a marginal decrease in ThT fluorescence was observed with $PNPase^{R398D/R399D}$, which also lacks phosphorolytic activity (37). These results indicate that ThT is applicable for evaluating the activities of RNA-metabolizing enzymes.

Determination of ADP concentrations using ThT and PNPase

The quantification of nucleotides (e.g. adenosine triphosphate and ADP) is usually performed using well-established methods such as the luciferin-luciferase reaction, coupled reactions of several metabolic enzymes-substrate sets (e.g. lactate dehydrogenase, pyruvate kinase, NADH and

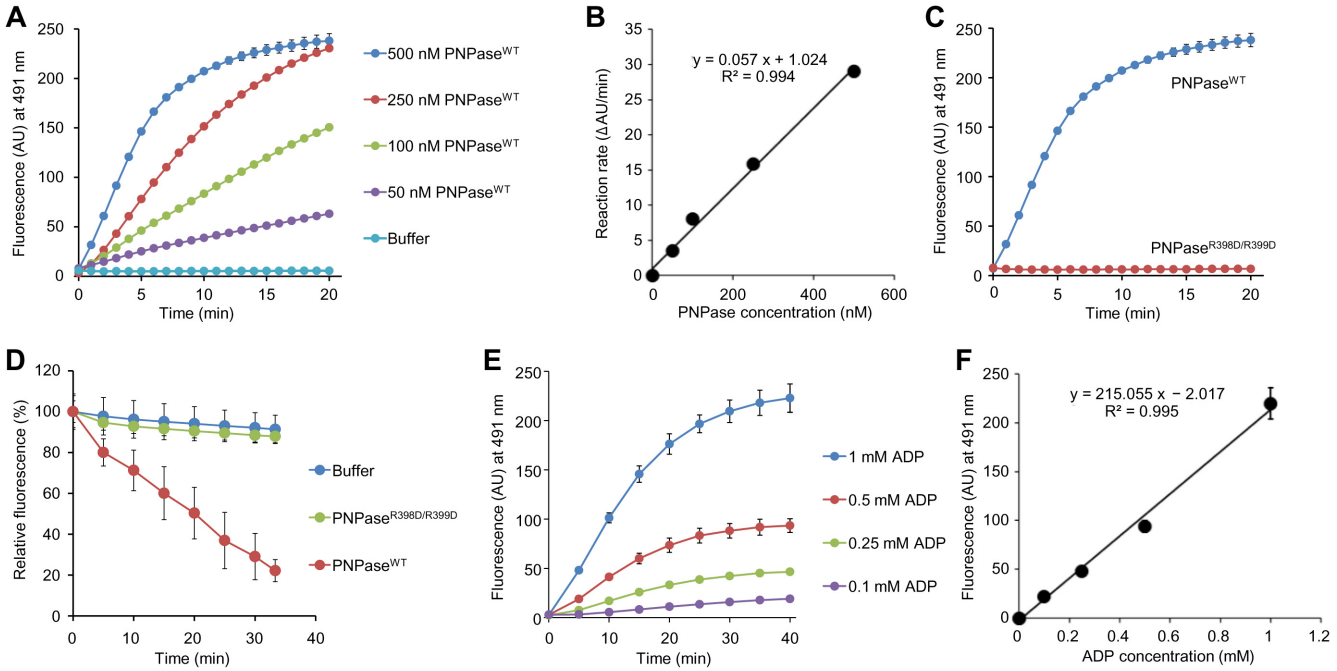

Figure 2. ThT is available for measuring activities of PNPase *in vitro*. (**A** and **B**) The kinetics and PNPase dose-dependency of poly(A) synthesis can be monitored at 25°C as a function of increase in ThT fluorescence. (**A**) The indicated concentrations of PNPase^{WT} were incubated with 1 mM ADP and 25 μM ThT and the real-time increases in fluorescence were recorded by spectrofluorometer. (**B**) The initial rates of the increase in the intensity (ΔAU/ml) were plotted against PNPase concentrations. The approximation line and its formula are shown with a correlation coefficient. (**C** and **D**) Poly(A) synthesis and degradation activities of PNPase^{WT} were compared with those of PNPase$^{R398D/R399D}$. (**C**) Poly(A) synthesis by 250 nM PNPase^{WT} or 250 nM PNPase$^{R398D/R399D}$ was monitored as described in (**A**). (**D**) Real-time changes of fluorescence intensity at 491 nm was monitored in the presence of 1 μM PNPase^{WT} or PNPase$^{R398D/R399D}$. (**E**) The kinetics and ADP dose-dependency of poly(A) synthesis can be monitored at 25°C in the presence of the indicated concentrations of ADP, 200 nM PNPase^{WT} and 25 μM ThT. (**F**) Fluorescence intensities recorded in (**E**) at 40 min were plotted against ADP concentrations. The approximation line and its formula are shown with a correlation coefficient. Data points represent the means and standard deviations of results from three independent experiments. The standard deviation is less than that corresponding to the size of the symbol if no error bars are seen.

phosphoenolpyruvate) (38), high performance liquid chromatography and capillary electrophoresis time of flight mass spectrometry (39). Given that poly(A) is synthesized from ADP by PNPase and that ThT binds to poly(A) in a concentration-dependent manner (Figure 1E and F), we hypothesized that ThT in combination with PNPase may be applicable for quantifying ADP in solution. To address this possibility, we incubated purified PNPase^{WT} at a fixed concentration (200 nM) with increasing ADP concentrations, ranging from 0.1 to 1 mM (Figure 2E). The maximum intensities of ThT fluorescence versus ADP concentration were estimated by linear regression, yielding a line equation of $y = 215.055x - 2.017$ and an R^2 value of 0.995 (Figure 2F), suggesting that ThT may be used in combination with PNPase to determine ADP concentrations in solution.

Application of ThT in monitoring RNA metabolism at a single-cell level

Our observation that ThT exhibited stronger fluorescence when bound to *E. coli* total RNA than *E. coli* genomic DNA (Figure 1A) prompted us to determine whether ThT can be used to monitor RNA metabolism *in vivo* at the single-cell level. First, we stained wild-type *E. coli* K-12 cells with ThT and observed intracellular staining of *E. coli* cells with ThT (Figure 3A). To clarify the subcellular localization of ThT-stained substances more precisely, we used an *E. coli* mutant harbouring the *ftsZ84* allele that forms a filamentous morphology in salt-free LB medium at 30°C, resulting in a widening of the cytoplasm (30,40). This characteristic allowed us to distinguish the cytoplasm from nucleoids in single cells (Figure 3B). Merged images clearly show that substances in the cytoplasmic space were stained with ThT. To address the possibility that the ThT-stained substances were in fact RNA molecules, we observed *E. coli* cells grown in the presence or absence of Rfp, an inhibitor of RNA polymerase. An overnight culture of *E. coli* cells grown in the presence of Rfp (0 h) showed minimal fluorescence, but high fluorescence intensities were observed with exponentially growing cells 1 and 5 h after the bacteria were switched to Rfp-free medium (Figure 3C). In contrast, the fluorescence of *E. coli* cells maintained in the presence of Rfp was very weak, as in the case of the overnight culture. Because *E. coli* mutant cells harbouring the *pnp-7* allele, in which cellular mRNA degradation activity would be decreased due to the lack of PNPase, showed stronger ThT fluorescence than wild-type cells (Supplementary Figure S6), it is most likely that the major substances stained with ThT in actively dividing cells were mRNAs.

To test this possibility unambiguously, *E. coli* cells expressing PNPase or its catalytic mutant (PNPase$^{R398D/R399D}$) were stained with ThT (Figure 4A). After induction of PNPase expression with IPTG, *E. coli* cells were incubated in the absence of Rfp on ice or

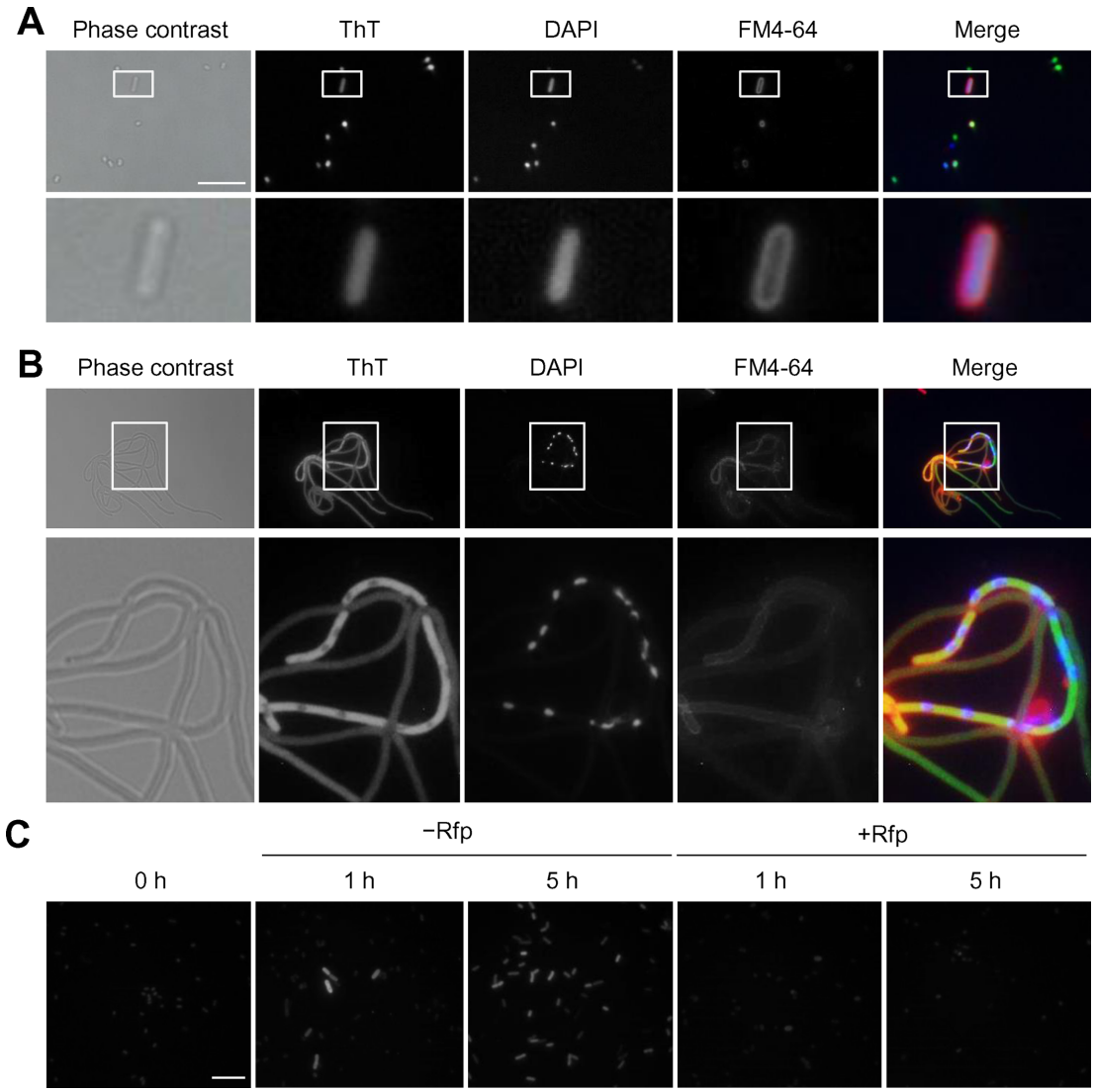

Figure 3. Cellular RNA metabolism can be monitored with ThT. (**A**) *Escherichiacoli* K-12 BW25113 cells grown in LB medium at 37°C for 16 h were stained with ThT (green), DAPI (blue), and FM4–64 (red) and the stained cells were observed under fluorescence microscopy. Phase contrast and fluorescence images are shown in grey scale and merged images are shown in original colours. (**B**) Log-phase cells of *E. coli* JEFZ1 containing the *ftsZ84* allele cultured in LB salt free medium at 37°C were also stained and observed similarly. (**C**) Overnight culture of BW25113 cells was transferred to fresh LB medium and incubated in the absence or presence of 100 μg/ml Rfp at 37°C. At the indicated time points, cells were harvested, stained with ThT and observed by fluorescence microscopy. Scale bars indicate 10 μm.

in the presence of Rfp at 37°C. Under the latter conditions where degradation of mRNA is stimulated by overexpressed PNPase and *de novo* mRNA synthesis is simultaneously blocked, ThT fluorescence is predicted to be lower than that observed under the former conditions. The fluorescence intensity of vector control cells in the presence of Rfp was modestly lower than that observed in the absence of Rfp (Figure 4B) due to the presence of endogenous PNPase and other ribonucleases in the cell. The difference of fluorescence intensity observed in the presence and absence of Rfp was pronounced in the case of $PNPase^{WT}$-expressing cells (Figure 4B and C). In addition, these cells showed lower fluorescence intensities in the absence of Rfp, compared to vector control cells, perhaps due to the presence of overexpressed PNPase (Figure 4D). $PNPase^{R398D/R399D}$-expressing cells also showed decreased fluorescence intensities in the presence of Rfp. However, their fluorescence intensities were higher than $PNPase^{WT}$-expressing cells, even though their expression levels were similar (Figure 4D). This observation likely reflects the decreased, but substantial phosphorolytic activity of this mutant PNPase (Figure 2D). These results suggest that most mRNAs were degraded by overexpressed $PNPase^{WT}$ when *de novo* mRNA synthesis was blocked by Rfp. In addition, we observed that deletion of the poly(A) synthetic enzyme-encoding gene *pcnB* (41) did not affect ThT binding to *E. coli* cells (Supplementary Figure S7) and that supplementation of the poly(A) binding protein Hfq did not lead to the increase in ThT fluorescence in the presence of poly(A) (Supplementary Figure S8), eliminating the

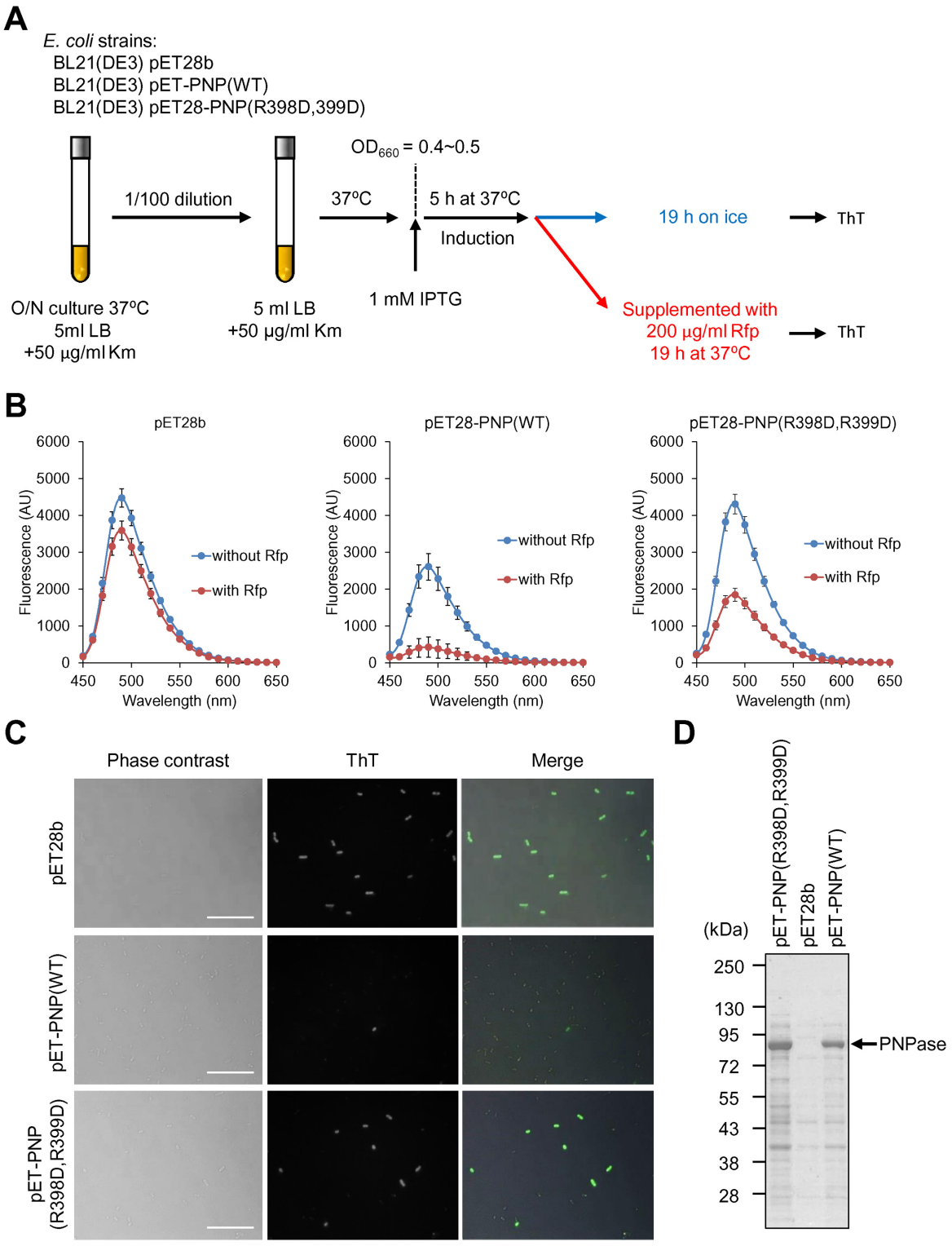

Figure 4. ThT is available for measuring RNA metabolic enzyme activities *in vivo*. (**A**) Experimental procedures are schematically described. Overnight culture of *Escherichia coli* strains were diluted 100-fold into fresh LB medium containing kanamycin (Km) and incubated until OD_{660} reached to 0.4–0.5. Subsequently the culture was supplemented with 1 mM IPTG and the expression of PNPase variants were induced at 37°C for 5 h. The culture was divided into two tubes; one of them was incubated on ice for 19 h and the other was supplemented with 200 μg/ml rifampicin (Rfp) and incubated at 37°C for 19 h. After removal of culture supernatant, equal wet weights of cells were suspended into PBS containing 25 μM ThT. ThT fluorescent spectra of the suspensions were measured using a spectrofluorometer (**B**), and cells were observed under fluorescence microscopy (**C**). (**B**) Data points represent the means and standard deviations of results from three independent experiments. The standard deviation is less than that corresponding to the size of the symbol if no error bars are seen. (**C**) Scale bars indicate 10 μm. (**D**) Expression of PNPase variants were checked by SDS-PAGE with CBB staining. Positions of molecular mass markers are represented at the left of the panel.

possibility that ThT binding is specific to poly(A) RNA or poly(A)-binding proteins interacting with poly(A) RNA in the cell. Taken together, these results strongly suggest that ThT can be used for monitoring mRNA levels (total transcriptome) in living single cells.

ThT staining visualizes transitions between normal cells and persister cells

We further evaluated the potential use of ThT for visualizing transitions between non-persister cells and persister cells, using the RpoS::mCherry translational fusion expression system that has been developed and evaluated as a potential tool for profiling persister cells at the single-cell level (11). In this system, persister cells coloured in red showed arrested growth and tolerance to multiple drugs (11). Using the ThT labelling method combined with the RpoS::mCherry fusion system, *E. coli* cells were rendered in three colours as follows: (i) green cells (ThT-positive, but RpoS::mCherry negative) are thought to be actively dividing with high mRNA levels and, therefore, to be non-persister cells; (ii) magenta cells (ThT-negative, but RpoS::mCherry positive cells) show overall low transcription levels, but RpoS::mCherry fusion is upregulated by stochastically induced (p)ppGpp (11) and, thus, thought to be persister cells; (iii) white cells, ThT- and RpoS::mCherry-positive, are considered to be transient-state cells (Figure 5A). During log-phase growth, numerous green cells (ThT-positive) and a low degree of magenta cells (RpoS::mCherry-positive) were observed (Figure 5B), indicating the presence of a minor population of persister cells at this growth phase. This observation is consistent with previously observed results (11). The time course of distribution and transition of non-persister cells to persister cells and *vice versa* were evaluated using this technique. In 4 and 7-h cultures corresponding to log and stationary-growth phases, respectively (Supplementary Figure S9), the majority of non-persister cells with high intensity of ThT fluorescence were observed, while persister cells were detected, but only rarely. A statistical analysis revealed that 11 cells out of 1007 analysed had elevated RpoS::mCherry levels. This data is consistent with data from a previously published study, wherein it was reported that 16 cells out of 1542 were RpoS::mCherry-fluorescence positive (11). During the transition from the early to late stationary growth phase, magenta-coloured RpoS::mCherry-positive cells became dominant (Figure 5C and Supplementary Figure S10; 7 h to 72 h). In the second round of cultivation, a large portion of magenta cells reverted to green cells at several hours after their transfer to fresh medium and then magenta cells predominated during stationary growth phase (Supplementary Figure S11). These results illustrate that ThT may have utility for profiling the transition of non-persister and persister cells at the single-cell level.

Use of ThT in probing RNA metabolic activity in various bacteria

In light of the intense interest in bacterial persistence, we next tested the possibility that mRNA metabolism in various bacteria can be evaluated using our ThT-probing method. Here, we tested several Gram-positive and Gram-negative bacteria, including *Staphylococcus aureus*, *Staphylococcus epidermidis*, *B. choshinensis*, *Pseudomonas aeruginosa*, *Vibrio cholerae* and *Klebsiella pneumoniae*. *S. aureus* and *S. epidermidis* are commensal Gram-positive cocci as well as opportunistic pathogens (42,43). *B. choshinensis* is a Gram-positive bacillus used for the production of secreted recombinant proteins (31). *P. aeruginosa* and *K. pneumoniae* are Gram-negative bacilli causing several infectious diseases (e.g. cystic fibrosis, pneumonia and blood-borne infections) (44–46). The cholera-causing agent *V. cholerae* is a Gram-negative, comma-shaped bacterium (47). All of the tested bacteria showed high fluorescence in the presence of ThT at mid-log growth phase, whereas their fluorescence intensities were decreased at the stationary phase (Figure 6). These profiles were similar to those of *E. coli* (Figure 5 and Supplementary Figures S10 and S11), strongly suggesting that actively dividing cells with high mRNA levels tend to be stainable with ThT and that the status of mRNAs in diverse bacteria can be monitored with this fluorescent probe.

DISCUSSION

Here, we established that ThT could be used as a fluorescent sensor to monitor mRNA levels *in vitro* and *in vivo*. One of the advantages of this approach is its simplicity. Conventionally, RNA synthesis and degradation have been analysed by polyacrylamide gel electrophoresis, radioisotope (RI)- or non-RI-labeled probes, and by alternative methods, as described previously (36,48). However, these approaches are complicated and time-consuming, making real-time monitoring of these reactions difficult. ThT becomes highly fluorescent only when bound to particular molecular entities such as amyloid fibrils and G-quadruplexes; thus, it offers a set of highly sensitive and convenient techniques for detecting cellular components and structures. In addition, ThT quantitatively fluoresces in the presence of RNA molecules, including poly(A), poly(G) and *E. coli* total RNA (Figure 1 and Supplementary Figure S1). These properties may be well suited for real-time quantitative analysis of RNA. To illustrate this point, we demonstrated that ThT can be used to monitor the time-course of poly(A) synthesis and its phosphorolysis triggered by PNPase *in vitro* (Figure 2). Given that ThT fluoresced more brightly when bound to $(A)_{50}$ compared to when bound to $(A)_{25}$ (Figure 1H), a minimal length of RNA molecules may be required for efficient ThT binding. As shown in Supplementary Figure S3, pre-heat treatment of $(A)_{50}$ at 90°C and more resulted in the reduced ThT-binding, suggesting a possibility that $(A)_{50}$ could form a certain secondary structure, such as parallel duplex (35), under the conditions used in this study.

We further established that ThT is applicable for monitoring mRNA levels in several living Gram-negative and Gram-positive bacterial cells and, thus, for visualizing transitions between non-persistent and persistent states at the single-cell level. Interestingly, all of the tested bacteria were stained strongly with ThT; however, the fluorescence intensities differed among different strains. The reason for the observed differences in fluorescence levels is not yet known. One possibility is that some bacteria such as *P. aeruginosa* use efflux pumps to transport ThT to the extracellular mi-

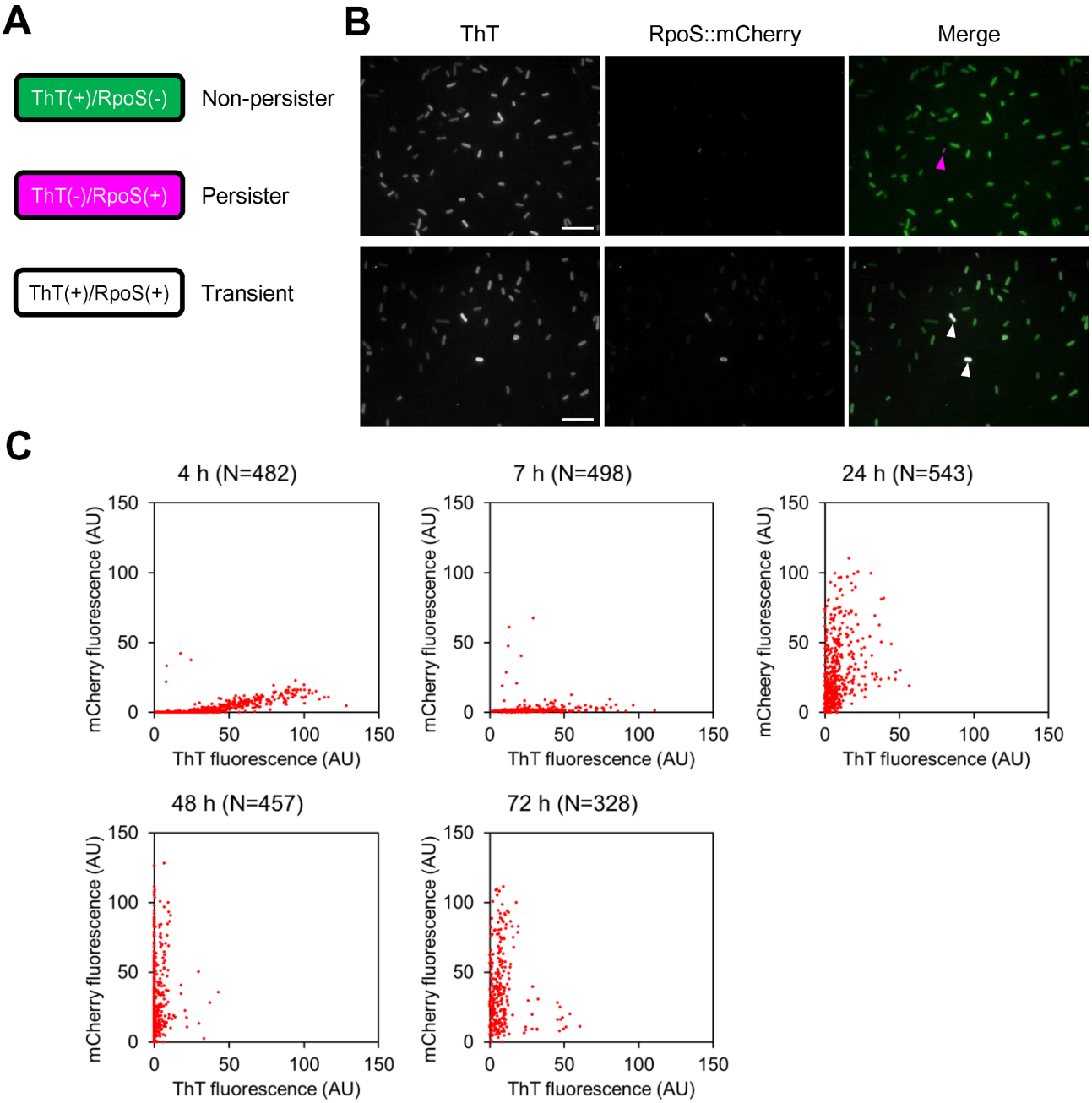

Figure 5. ThT is applicable for visualizing transitions between non-persister cells and persister cells. (**A**) Using an RpoS::mCherry reporter system, persister cells can be distinguished from non-persister cells as red fluorescent cells (pseudo-coloured in magenta). Non-persister cells are actively dividing and their mRNA level may be high enough for representing bright ThT fluorescence (green) in the presence of the fluorescence probe. Transient state cells (from non-persister to persister state or *viceversa*) are thought to exhibit green and magenta and are therefore in white when both fluorescence images are merged. (**B**) ThT fluorescence and mCherry fluorescence images of *Escherichia coli* MG1655 *rpoS::mcherry* cells at log phase (4 h) are shown in grey scale. These images are merged in the right panel. Many green cells and a few magenta cells are observed at the indicated time points. Magenta and white arrowheads represent ThT-negative/RpoS::mCherry-positive (persister) and ThT-positive/RpoS::mCherry-positive (transient) cells, respectively. Scale bars represent 10 μm. (**C**) *E. coli* MG1655 *rpoS::mcherry* cells were harvested and observed under fluorescence microscopy at the indicated periods. Intensities of ThT fluorescence and mCherry fluorescence of individual cells were quantified using Image J and plotted. Growth curve and microscopic images of the strain are shown in Supplementary Figures S5 and S6, respectively.

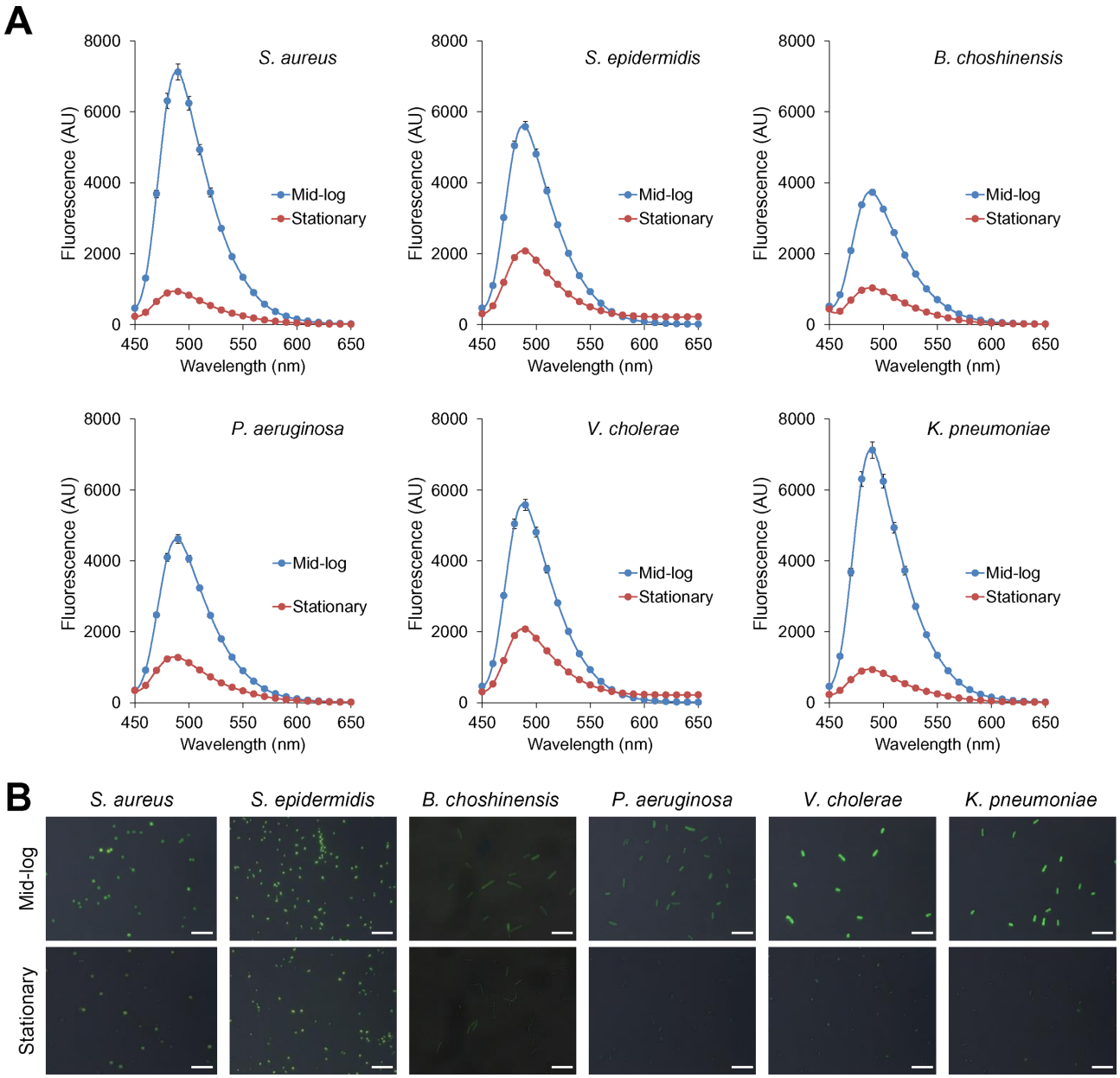

Figure 6. ThT stains various bacterial cells in a growth-phase-dependent manner. (**A**) Gram-positive (*Staphylococcus aureus*, *Staphylococcus epidermidis* and *Brevibacillus choshinensis*) and Gram-negative bacterial cells (*Pseudomonas aeruginosa*, *Vibrio cholerae* and *Klebsiella pneumoniae*) were harvested at the mid-log (3–5 h) and stationary phases (24 h) and were suspended into PBS containing 25 μM ThT. Fluorescence spectra were recorded with excitation at 438 nm. Data points represent the means and standard deviations of results from three independent experiments. The standard deviation is less than that corresponding to the size of the symbol if no error bars are seen. (**B**) Fluorescence and phase contrast images of the indicated bacteria are captured in the presence of ThT. Merged images of ThT fluorescence and phase contrast images are shown. Scale bars represent 10 μm.

lieu, as they do with antibiotics (49). Another possibility is that mRNA levels in certain bacteria may be intrinsically lower than in other bacteria. ThT-fluorescence levels could also differ among strains even in single species. Addressing these possibilities may lead to an enhanced understanding of the basic principles and evolution of bacterial RNA metabolism and regulation.

In addition, ThT at concentrations of 10 μM and lower did not affect bacterial growth, including that of *E. coli* (Supplementary Figure S12A) and other bacteria (Supplementary Figure S13). The observation that bacterial cells grew robustly in the presence of effective ThT concentrations (Figures 6 and Supplementary Figure S12B) illustrates the potential use of ThT in live cell imaging. Furthermore, given the intense interest in bacterial persistence and in expanding the scope of target bacteria, the ease and reproducibility of our assay should have broad applications in bacterial physiology. This method may also advance the conventional uses of the amyloid-binding compounds for basic research and diagnostic purposes in the realm of drug discovery screening. ThT binds to RNA as well as amyloid fibrils and G-quadruplexes, while ThS binds only to amy-

loid fibrils but neither RNA nor G-quadruplexes (Supplementary Figure S2). Thus, it is promising that ThT derivatives can be developed with more strict specificities, e.g. an RNA-specific derivative that does not bind amyloids or G-quadruplexes. Such derivatives should provide new insights into RNA metabolism, as well as amyloid biology.

SUPPLEMENTARY DATA

Supplementary Data are available at NAR online.

ACKNOWLEDGEMENTS

We thank Dr K. Gerdes (Department of Biology, University of Copenhagen) for providing *E. coli* MG1655 *rpoS::mcherry* and for his critical evaluation of the manuscript and valuable suggestions, which improved the quality of this manuscript. We are also grateful to Drs B. Bukau, A. Mogk and Y. Oguchi (Zentrum für Molekulare Biologie der Universität Heidelberg) for assisting in the construction of PNPase mutants.

FUNDING

Grant-in-Aid for Scientific Research [08J01771 to S.S.]; Excellent Young Researchers Overseas Visit Program [to S.S.]; Japan Society for the Promotion of Science (JSPS), Grant-in-Aid for Young Scientists (B) [24780079 to S.S.]; Joint Usage/Research Center for Developmental Medicine, IMEG, Kumamoto University; MEXT-Supported Program for the Strategic Research Foundation at Private Universities, 2012–2016 [to Y.M.]; JSPS Research Fellowship [to S.S.]. Funding for open access charge: JSPS, Grant-in-Aid for Young Scientists (B) [24780079].
Conflict of interest statement. None declared.

REFERENCES

1. Elowitz,M.B., Levine,A.J., Siggia,E.D. and Swain,P.S. (2002) Stochastic gene expression in a single cell. *Science*, **297**, 1183–1186.
2. Ozbudak,E.M., Thattai,M., Kurtser,I., Grossman,A.D. and van Oudenaarden,A. (2002) Regulation of noise in the expression of a single gene. *Nat. Genet.*, **31**, 69–73.
3. Blake,W.J., KAErn,M., Cantor,C.R. and Collins,J.J. (2003) Noise in eukaryotic gene expression. *Nature*, **422**, 633–637.
4. Kussell,E. and Leibler,S. (2005) Phenotypic diversity, population growth, and information in fluctuating environments. *Science*, **309**, 2075–2078.
5. Süe,G.M., Kulkarni,R.P., Dworkin,J., Garcia-Ojalvo,J. and Elowitz,M.B. (2007) Tunability and noise dependence in differentiation dynamics. *Science*, **315**, 1716–1719.
6. Wang,L., Brugge,J.S. and Janes,K.A. (2011) Intersection of FOXO- and RUNX1-mediated gene expression programs in single breast epithelial cells during morphogenesis and tumor progression. *Proc. Natl. Acad. Sci. U.S.A.*, **108**, E803–E812.
7. Golding,I. and Cox,E.C. (2004) RNA dynamics in live *Escherichia coli* cells. *Proc. Natl. Acad. Sci. U.S.A.*, **101**, 11310–11315.
8. Golding,I., Paulsson,J., Zawilski,S.M. and Cox,E.C. (2005) Real-time kinetics of gene activity in individual bacteria. *Cell*, **123**, 1025–1036.
9. Valencia-Burton,M., McCullough,R.M., Cantor,C.R. and Broude,N.E. (2007) RNA visualization in live bacterial cells using fluorescent protein complementation. *Nat. Methods*, **4**, 421–427.
10. Montero Llopis,P., Jackson,A.F., Sliusarenko,O., Surovtsev,I., Heinritz,J., Emonet,T. and Jacobs-Wagner,C. (2010) Spatial organization of the flow of genetic information in bacteria. *Nature*, **466**, 77–81.
11. Maisonneuve,E., Castro-Camargo,M. and Gerdes,K. (2013) (p)ppGpp controls bacterial persistence by stochastic induction of toxin-antitoxin activity. *Cell*, **154**, 1140–1150.
12. Maisonneuve,E. and Gerdes,K. (2014) Molecular mechanisms underlying bacterial persisters. *Cell*, **157**, 539–548.
13. Bigger,J. (1944) Treatment of staphylococcal infections with penicillin by intermittent sterilization. *Lancet*, **244**, 497–500.
14. Allison,K.R., Brynildsen,M.P. and Collins,J.J. (2011) Metabolite-enabled eradication of bacterial persisters by aminoglycosides. *Nature*, **473**, 216–220.
15. Nguyen,D., Joshi-Datar,A., Lepine,F., Bauerle,E., Olakanmi,O., Beer,K., McKay,G., Siehnel,R., Schafhauser,J., Wang,Y. *et al.* (2011) Active starvation responses mediate antibiotic tolerance in biofilms and nutrient-limited bacteria. *Science*, **334**, 982–986.
16. Conlon,B.P., Nakayasu,E.S., Fleck,L.E., LaFleur,M.D., Isabella,V.M., Coleman,K., Leonard,S.N., Smith,R.D., Adkins,J.N. and Lewis,K. (2013) Activated ClpP kills persisters and eradicates a chronic biofilm infection. *Nature*, **503**, 365–370.
17. Wakamoto,Y., Dhar,N., Chait,R., Schneider,K., Signorino-Gelo,F., Leibler,S. and McKinney,J.D. (2013) Dynamic persistence of antibiotic-stressed mycobacteria. *Science*, **339**, 91–95.
18. Maisonneuve,E., Shakespeare,L.J., Jørgensen,M.G. and Gerdes,K. (2011) Bacterial persistence by RNA endonucleases. *Proc. Natl. Acad. Sci. U.S.A.*, **108**, 13206–13211.
19. Helaine,S. and Holden,D.W. (2013) Heterogeneity of intracellular replication of bacterial pathogens. *Curr. Opin. Microbiol.*, **16**, 184–191.
20. Helaine,S., Cheverton,A.M., Watson,K.G., Faure,L.M., Matthews,S.A. and Holden,D.W. (2014) Internalization of *Salmonella* by macrophages induces formation of nonreplicating persisters. *Science*, **343**, 204–208.
21. Biancalana,M. and Koide,S. (2010) Molecular mechanism of Thioflavin-T binding to amyloid fibrils. *Biochim. Biophys. Acta*, **1804**, 1405–1412.
22. Naiki,H., Higuchi,K., Hosokawa,M. and Takeda,T. (1989) Fluorometric determination of amyloid fibrils in vitro using the fluorescent dye, thioflavin T1. *Anal. Biochem.*, **177**, 244–249.
23. LeVine,H. III (1993) Thioflavine T interaction with synthetic Alzheimer's disease beta-amyloid peptides: detection of amyloid aggregation in solution. *Protein Sci.*, **2**, 404–410.
24. Gabelica,V., Maeda,R., Fujimoto,T., Yaku,H., Murashima,T., Sugimoto,N. and Miyoshi,D. (2013). Multiple and cooperative binding of fluorescence light-up probe thioflavin T with human telomere DNA G-quadruplex. *Biochemistry*, **52**, 5620–5628.
25. Mohanty,J., Barooah,N., Dhamodharan,V., Harikrishna,S., Pradeepkumar,P.I. and Bhasikuttan,A.C. (2013) Thioflavin T as an efficient inducer and selective fluorescent sensor for the human telomeric G-quadruplex DNA. *J. Am. Chem. Soc.*, **135**, 367–376.
26. Renaud de la Faverie,A., Guédin,A., Bedrat,A., Yatsunyk,L.A. and Mergny,J.L. (2014) Thioflavin T as a fluorescence light-up probe for G4 formation. *Nucleic Acids Res.*, **42**, e65.
27. Burge,S., Parkinson,G.N., Hazel,P., Todd,A.K. and Neidle,S. (2006) Quadruplex DNA: sequence, topology and structure. *Nucleic Acids Res.*, **34**, 5402–5415.
28. Reiner,A.M. (1969) Isolation and mapping of polynucleotide phosphorylase mutants of *Escherichia coli*. *J. Bacteriol.*, **97**, 1431–1436.
29. Arraiano,C.M., Yancey,S.D. and Kushner,S.R. (1988) Stabilization of discrete mRNA breakdown products in *ams pnp rnb* multiple mutants of *Escherichia coli* K-12. *J. Bacteriol.*, **170**, 4625–4633.
30. Jung,H.K., Ishino,F. and Matsuhashi,M. (1989). Inhibition of growth of *ftsQ*, *ftsA*, and *ftsZ* mutant cells of *Escherichia coli* by amplification of a chromosomal region encompassing closely aligned cell division and cell growth genes. *J. Bacteriol.*, **171**, 6379–6382.
31. Sugimoto,S., Iwase,T., Sato,F., Tajima,A., Shinji,H. and Mizunoe,Y. (2011) Cloning, expression and purification of extracellular serine protease Esp, a biofilm-degrading enzyme, from *Staphylococcus epidermidis*. *J. Appl. Microbiol.*, **111**, 1406–1415.
32. Sugimoto,S., Saruwatari,K., Higashi,C. and Sonomoto,K. (2008) The proper ratio of GrpE to DnaK is important for protein quality control by the DnaK-DnaJ-GrpE chaperone system and for cell division. *Microbiology*, **154**, 1876–1885.
33. Sugimoto,S., Higashi,C., Saruwatari,K., Nakayama,J. and Sonomoto,K. (2007) A gram-negative characteristic segment in

Escherichia coli DnaK is essential for the ATP-dependent cooperative function with the co-chaperones DnaJ and GrpE. *FEBS Lett.*, **581**, 2993–2999.
34. Sugimoto,S., Higashi,C., Yoshida,H. and Sonomoto,K. (2008) Construction of *Escherichia coli dnaK*-deletion mutant infected by λDE3 for overexpression and purification of recombinant GrpE proteins. *Protein Expr. Purif.*, **60**, 31–36.
35. Safaee,N., Noronha,A.M., Rodionov,D., Kozlov,G., Wilds,C.J., Sheldrick,G.M. and Gehring,K. (2013) Structure of the parallel duplex of poly(A) RNA: evaluation of a 50 year-old prediction. *Angew. Chem. Int. Ed. Engl.*, **52**, 10370–10373.
36. Carpousis,A.J., Van Houwe,G., Ehretsmann,C. and Krisch,H.M. (1994) Copurification of *E. coli* RNAase E and PNPase: evidence for a specific association between two enzymes important in RNA processing and degradation. *Cell*, **76**, 889–900.
37. Jarrige,A., Bréchemier-Baey,D., Mathy,N., Duché,O. and Portier,C. (2002) Mutational analysis of polynucleotide phosphorylase from *Escherichia coli*. *J. Mol. Biol.*, **321**, 397–409.
38. Nishikori,S., Esaki,M., Yamanaka,K., Sugimoto,S. and Ogura,T. (2011) Positive cooperativity of the p97 AAA ATPase is critical for essential functions. *J. Biol. Chem.*, **286**, 15815–15820.
39. Hironaka,I., Iwase,T., Sugimoto,S., Okuda,K., Tajima,A., Yanaga,K. and Mizunoe,Y. (2013) Glucose triggers ATP secretion from bacteria in a growth-phase-dependent manner. *Appl. Environ. Microbiol.*, **79**, 2328–2335.
40. Addinall,S.G., Cao,C. and Lutkenhaus,J. (1997) Temperature shift experiments with an *ftsZ84*(Ts) strain reveal rapid dynamics of FtsZ localization and indicate that the Z ring is required throughout septation and cannot reoccupy division sites once constriction has initiated. *J. Bacteriol.*, **179**, 4277–4284.
41. Cao,G.J. and Sarkar,N. (1992) Identification of the gene for an *Escherichia coli* poly(A) polymerase. *Proc. Natl. Acad. Sci. U.S.A.*, **89**, 10380–10384.
42. von Eiff,C., Becker,K., Machka,K., Stammer,H. and Peters,G. (2001) Nasal carriage as a source of *Staphylococcus aureus* bacteremia. Study Group. *N. Engl. J. Med.*, **344**, 11–16.
43. Sugimoto,S., Iwamoto,T., Takada,K., Okuda,K., Tajima,A., Iwase,T. and Mizunoe,Y. (2013) *Staphylococcus epidermidis* Esp degrades specific proteins associated with *Staphylococcus aureus* biofilm formation and host-pathogen interaction. *J. Bacteriol.*, **195**, 1645–1655.
44. Jones,A.M., Govan,J.R., Doherty,C.J., Dodd,M.E., Isalska,B.J., Stanbridge,T.N. and Webb,A.K. (2001) Spread of a multiresistant strain of *Pseudomonas aeruginosa* in an adult cystic fibrosis clinic. *Lancet*, **358**, 557–558.
45. Rowe,S.M., Miller,S. and Sorscher,E.J. (2005) Cystic fibrosis. *N. Engl. J. Med.*, **352**, 1992–2001.
46. Peleg,A.Y. and Hooper,D.C. (2010) Hospital-acquired infections due to gram-negative bacteria. *N. Engl. J. Med.*, **362**, 1804–1813.
47. Sack,D.A., Sack,R.B., Nair,G.B. and Siddique,A.K. (2004) Cholera. *Lancet*, **363**, 223–233.
48. Regonesi,M.E., Briani,F., Ghetta,A., Zangrossi,S., Ghisotti,D., Tortora,P. and Dehò,G. (2004) A mutation in polynucleotide phosphorylase from *Escherichia coli* impairing RNA binding and degradosome stability. *Nucleic Acids Res.*, **32**, 1006–1017.
49. Nikaido,H. (1994) Prevention of drug access to bacterial targets: permeability barriers and active efflux. *Science*, **264**, 382–388.